Finally, considering possible interchain interactions, one notes that the closest approach of the two different types of chains is about the same as the closest approach between the $(MnCl_4)^{2-}$ tetrahedral chains. It thus seems likely that interchain interactions between the two different types of chains will be responsible for any long-range transition which occurs in $[(CH_3)_3NH]_3Mn_2Cl_7$. Because of the small intrachain exchange in the tetrahedral chains, it would seem that there is a reasonable possibility that such a transition will occur at a lower temperature than the one observed in TMMC. In any case, lower temperature measurements should provide useful insight into the interchain interactions and may well prove $[(CH_3)_3NH]_3Mn_2Cl_7$ to be a more ideal one-dimensional material than TMMC.

Acknowledgment. The support of this work by the UICC Research Board is appreciated, as is the cooperation of the UICC computer center in supplying computer time. The author wishes to thank Dr. R. D. Willett for communicating some of his results prior to publication. The cooperation of Drs. R. Caputo, S. Roberts, R. D. Willett, and B. C. Gerstein in agreeing to delay publication of their work[8] so this paper could appear simultaneously is also appreciated.

Registry No. $[(CH_3)_3NH]_3Mn_2Cl_7$, 58150-41-7.

References and Notes

(1) L. J. de Jongh and A. R. Miedema, *Adv. Phys.*, **23**, 1 (1974).
(2) See, e.g., S. Merchant, J. N. McElearney, G. E. Shankle, and R. L. Carlin, *Physica (Utrecht)*, **78**, 308 (1974).
(3) R. M. Clay, P. Murray-Rust, and J. Murray-Rust, *J. Chem. Soc., Dalton Trans.*, 595 (1973).
(4) R. Dingle, M. E. Lines, and S. L. Holt, *Phys. Rev.*, **187**, 643 (1969).
(5) L. R. Walker, R. E. Dietz, K. Andres, and S. Darack, *Solid State Commun.*, **11**, 593 (1972).
(6) M. T. Hutchings, G. Shirane, R. J. Birgeneau, and S. L. Holt, *Phys. Rev. B*, **5**, 1999 (1972).
(7) R. E. Dietz, F. R. Merritt, R. Dingle, D. Hone, B. G. Silbernagel, and P. M. Richards, *Phys. Rev. Lett.*, **26**, 1186 (1971).
(8) R. Caputo, S. Roberts, R. D. Willett, and B. C. Gerstein, *Inorg. Chem.*, preceding paper in this issue.
(9) J. N. McElearney, D. B. Losee, S. Merchant, and R. L. Carlin, *Phys. Rev. B*, **7**, 3314 (1973).
(10) T. Smith and S. A. Friedberg, *Phys. Rev.*, **176**, 660 (1968).
(11) J. W. Stout and W. B. Hadley, *J. Chem. Phys.*, **40**, 55 (1964).
(12) M. E. Fisher, *Proc. R. Soc. London, Ser. A*, **254**, 66 (1960).
(13) J. N. McElearney, S. Merchant, G. E. Shankle, and R. L. Carlin, *J. Chem. Phys.*, in press.
(14) Y. Tazuke and K. Nagata, *J. Phys. Soc. Jpn.*, **38**, 1003 (1975).
(15) H. W. White, K. H. Lee, J. Trainor, D. C. McCollum, and S. L. Holt, *AIP Conf. Proc.*, **No. 18**, 376 (1973).
(16) K. Takeda, *Phys. Lett. A*, **47**, 335 (1974).
(17) R. E. Dietz, L. R. Walker, F. S. L. Hsu, W. H. Haemmerle, B. Vis, C. K. Chau, and H. Weinstock, *Solid State Commun.*, **15**, 1185 (1974).
(18) B. Vis, C. K. Chau, H. Weinstock, and R. E. Dietz, *Solid State Commun.*, **15**, 1765 (1974).
(19) K. Kopinga, T. de Neef, and W. J. M. de Jonge, *Phys. Rev. B*, **11**, 2364 (1975).

Contribution from the Department of Chemistry,
The University of Wyoming, Laramie, Wyoming 82071

Physical Properties of Linear-Chain Systems. III. Absorption Spectra of $RbFeBr_3$, $CsFeBr_3$, $RbFeCl_3$, $CsFeCl_3$, and $CsMg_{1-x}Fe_xCl_3$

CHARLES F. PUTNIK, G. MATTNEY COLE, Jr., B. B. GARRETT,[1] and SMITH L. HOLT*

Received October 7, 1975 AIC50734E

The polarized, single-crystal absorption spectra of the linear-chain compounds $RbFeBr_3$, $CsFeBr_3$, $RbFeCl_3$, $CsFeCl_3$, and $CsMg_{1-x}Fe_xCl_3$ have been measured between 298 and 4.2 K. The spectra of the pure salts and the dilute samples are similar in terms of absorption positions but the spin-forbidden transitions in the pure salts show anomalous intensity. The intensity of spin-forbidden absorptions in some cases nearly equals that of the spin-allowed $^5T_2(D) \rightarrow {}^5E(D)$ absorption. The spectra are assigned to the octahedral, ligand field states of the high-spin d^6 electronic configuration. The intensity of the spin-forbidden transitions results from a cooperative mechanism which relaxes the spin selection rule without energetically perturbing the electronic states involved. The results of this work add significant features to the empirical characterization of this mechanism and may aid theoretical progress in this area.

Introduction

The unusual physical properties displayed by certain materials of the ABX_3 formulation derive from the unique structure of these compounds. When $A^+ = Cs^+$, Rb^+, or $(CH_3)_4N^+$, B = a divalent, first-row transition metal ion, and $X^- = Cl^-$, Br^-, or I^-, these materials crystallize as a hexagonal array of infinite linear chains of face-sharing $[X_3BX_3]^{4-}$ octahedra separated by the A cations. The interchain separation afforded by the A cations acts as an effective magnetic insulation which constrains exchange interactions to one dimension, that along the chains.[2]

The unique character of these systems is evidenced in their magnetic and spectral properties. Tetramethylammonium trichloromanganate(II), TMMC, orders in three dimensions only at 0.84 K[3] while spin correlation in one dimension is evident at much higher temperatures.[4] Measured absorption spectra reveal a cooperative mechanism which relaxes the $\Delta S = 0$ spin selection rule and results in marked enhancement of absorptions corresponding to formally spin-forbidden transitions.[3,5–7] Such enhancement is observed in materials which possess isotropic exchange coupling but appears to be most pronounced in the ABX_3 linear-chain materials.

In an effort to characterize these unique compounds more fully and to resolve better the effect of unidimensional magnetic exchange on the electronic properties of the system, the absorption spectra of $RbFeBr_3$, $CsFeBr_3$, $RbFeCl_3$, $CsFeCl_3$, and $CsMg_xFe_{1-x}Cl_3$ have been investigated between room temperature and 4.2 K. $CsFeCl_3$[8] and $RbFeCl_3$[8–10] are reported to possess intrachain ferromagnetic coupling and interchain antiferromagnetic coupling with $T_N < 1.3$ K and $T_N = 2.54$ K, respectively. $RbFeBr_3$ is reported to possess intrachain and interchain antiferromagnetic coupling with $T_N = 5.5$ K. The magnetic properties of $CsFeBr_3$ have not been studied in detail but measurements of powder susceptibility between room temperature and 4.2 K correlate well with those of $RbFeBr_3$.[12] Thus, these materials provide a means of comparing the effects of ferromagnetic and antiferromagnetic intrachain exchange coupling on the absorption spectra of isoelectronic, isostructural materials.

This study also serves a second fundamental purpose by providing a better empirical characterization of the triplet structure of iron(II). The electronic structure of this ion in an octahedral field is dominated by spin-forbidden $^5T_2(D) \rightarrow {}^3\Gamma$ transitions with only one quintet–quintet excitation possible.

Because the excited quintet state is subject to a dynamic Jahn–Teller distortion, the spin-allowed, $^5T_2(D) \rightarrow {}^5E(D)$, transition has received the majority of attention.[13-18] Other investigators have examined side bands in the FeF_2 spectrum[19-21] and only Ferguson et al. in their study of $RbFeF_3$[22] have treated the triplet levels in any detail. However, in this latter work measurements were carried out at 77 K where significant overlap complicates the spectral assignment. The strong enhancement of the triplet absorptions in the spectra of the $AFeX_3$ materials facilitates assignment of these states and comparison of the spectra provides a useful empirical characterization of the mechanism of enhancement.

Experimental Section

Preparation. Anhydrous $FeCl_2$ was prepared by heating Mallinckrodt AR grade $FeCl_2{\cdot}4H_2O$ at 250 °C in a stream of dry HCl gas. Anhydrous $FeBr_2$ (Great Western Inorganics), CsCl, RbCl, CsBr, RbBr (ROC/RIC), and $MgCl_2$ (Ventron) were purchased at 99+% purity and all compounds were purified further by zone refining. The compounds $CsFeCl_3$, $RbFeCl_3$, $CsFeBr_3$, and $RbFeBr_3$ were prepared by mixing equimolar quantities of the appropriate alkali halide and iron(II) halide, sealing the mixture in an evacuated quartz ampule, and refining via a modified Bridgman method. $CsMgCl_3$ was prepared in the analogous manner and combined with the appropriate molar quantity of $CsFeCl_3$ to produce the compounds $CsMg_{0.95}Fe_{0.05}Cl_3$ and $CsMg_{0.88}Fe_{0.12}Cl_3$. (Exact concentrations were determined spectroscopically.)

In this manner, single-crystal boules ~5 cm in length and 1.5 cm in diameter were produced. From these it was possible to cleave sections suitable for σ, π, and axial spectroscopic measurements. The crystals cleaved easily in planes parallel to the c axis but cleavage perpendicular to the c axis was difficult and the axial samples required careful polishing with a 95:5 methanol–water solution.

When viewed with unpolarized light, crystalline samples of $CsFeCl_3$, $RbFeCl_3$, $CsFeBr_3$, and $RbFeBr_3$ appeared deep brown-amber. However, when observed with polarized light, the compounds appeared deep red when the plane of polarization was parallel to the c axis and pale yellow when the plane of polarization was perpendicular to the c axis. The magnesium compounds containing small percentages of iron(II) appeared faint brown-amber in unpolarized light, pale pink when viewed with plane-polarized light parallel to the c axis, and very pale yellow when the plane of polarization was perpendicular to the c axis.

Crystal Structures. $CsFeCl_3$,[23] $RbFeCl_3$,[23] $RbFeBr_3$,[24,25] and $CsMgCl_3$[26] are isomorphous and belong to the hexagonal space group $P6_3/mmc$. The cell dimensions are a = 7.24, 7.06, 7.38, and 7.27 Å and c = 6.05, 6.02, 6.28, and 6.19 Å, respectively. The structure consists of linear chains of face-sharing $[FeX_6]^{4-}$ or $[MgCl_6]^{4-}$ octahedra separated by the alkali cations. The transition metal ion site symmetry is D_{3d}. The structure of $CsFeBr_3$ has not been reported; however preliminary x-ray powder diffraction measurements indicate this compound possesses the same structure.[27]

Spectroscopic Measurements. The σ and π, single-crystal absorption spectra of $CsFeCl_3$, $CsFeBr_3$, $RbFeCl_3$, and $RbFeBr_3$ were measured at 298, 150, 77, 40, 20, and 4.2 K in the spectral range 4500–30000 cm^{-1}. The axial spectra were measured over the same range and were found to be identical with the σ measurements indicating all transitions are of electric dipole nature. The σ and π spectral measurements of $CsMg_{1-x}Fe_xCl_3$ were made at 298, 77, and 4.2 K in the range 4500–34000 cm^{-1}. All spectra were measured using a Cary Model 14-RI recording spectrophotometer. The single crystals were mounted on aluminum rings which were inserted into the sample chamber of an Oxford Cf-100 cryostat. Temperature was determined and controlled to within ±2 K with an Oxford VC-30 temperature controller. Polarized spectra were obtained by inserting Glan-Thompson prisms in the light paths of the spectrometer's sample and reference compartments. Oscillator strengths were determined as previously described.[28] The error in this method is estimated to be less than 10%.

Table I

$RbFeCl_3$ obsd energies, cm^{-1}		$CsFeCl_3$ obsd energies, cm^{-1}		Calcd energies, cm^{-1} [a]	Assignment
$E \parallel c$	$E \perp c$	$E \parallel c$	$E \perp c$		
6 803	6 850	6 400	6.211		
7 519	7 576	7 350	7 350	7 250	$^5E(D)$
12 346	12 157	12 658	12 346	11 993	$^3T_1(H)$[a]
		14 599			
15 152	15 106	15 207	15 378		
		15 444			
		15 686		16 671	$^3T_2(H)$
~18 200	18 182	~18 300	18 250		
19 128		19 186			
19 354	19 357	19 410	~19 250	19 649	$^3T_1(P)$
20 182	20 157	20 206	20 161	20 167	$^3T_1(H)$[b]
21 142	21 133	21 169	21 142	21 342	$^3T_2(F)$
21 872	21 805	21 810	21 834		
~22 625		~22 700		22 252	$^3E(H)$
23 213	23 242	23 288	23 250		
23 419	23 359	23 379	23 425		
23 923	23 469	23 463	23 474		
	23 940	23 923	23 981		
	24 115	24 114			
		24 190	24 155		
				26 116	$^3T_2(G)$

[a] $Dq = 725$ cm^{-1}; $B = 875$ cm^{-1}; $C = 3800$ cm^{-1}.

Table II

$RbFeBr_3$ obsd energies, cm^{-1}		$CsFeBr_3$ obsd energies, cm^{-1}		Calcd energies, cm^{-1} [a]	Assignment
$E \parallel c$	$E \perp c$	$E \parallel c$	$E \perp c$		
5 848	5 882	5 525	5 495		
6 711	6 711	6 589	6 661	6 500	$^5E(D)$
12 048	12 048	12 422	12 195	11 800	$^3T_1(H)$[a]
14 699	14 815	15 267	15 152		
				16 357	$^3T_2(H)$
17 277	17 153		17 191		
17 575	17 730	17 699	17 687		
	18 116				
18 437		18 471			
18 584		18 660			
18 702	18 691	18 737	18 748		
18 847		18 888		18 931	$^3T_1(P)$
19 026	19 004	19 060	19 073		
19 209	19 157	19 305	19 220	19 333	$^3T_1(H)$[b]
19 342		19 433			
19 685	19 654	19 697	19 673		
		20 243	20 243		
20 387	20 445	20 479	20 492		
20 781	20 759	20 768	20 756	20 789	$^3T_2(F)$
21 368	21 119	21 137	21 160		
		21 400		21 453	$^3E(H)$
		21 950			
	22 583		22 609		
22 799	22 768		22 805		
22 899	22 999		22 946		
	23 148		23 191		
	23 397		23 419		
				25 177	$^3T_2(G)$

[a] $Dq = 650$ cm^{-1}; $B = 900$ cm^{-1}; $C = 3600$ cm^{-1}.

Results

In terms of general appearance and absorption positions the spectra of $RbFeBr_3$, $CsFeBr_3$, $RbFeCl_3$, $CsFeCl_3$, and $CsMg_{0.88}Fe_{0.12}Cl_3$ are similar and are shown in Figures 1–5, respectively. The spectrum of $CsMg_{0.95}Fe_{0.05}Cl_3$ is also shown in Figure 5 but is of such low intensity above ~10000 cm^{-1} that determination of absorption positions is difficult and ambiguous. The observed energy levels of the other systems are listed in Tables I–III. The spectra are characterized by five absorption regions. The region from 4500 to 10000 cm^{-1} contains a broad, intense, asymmetric band attributable in all of the compounds to the spin-allowed $^5T_2 \rightarrow {}^5E$ transition. It is the most intense region in the spectra of the dilute samples. This band decreases in oscillator strength by between 10% and 30%, depending on the compound, as the temperature is lowered from 298 to 77 K. Below 77 K the oscillator strengths remain constant within experimental error. This behavior parallels that of a vibronically assisted transition. The os-

Table III

$CsMg_{0.88}Fe_{0.12}Cl_3$ obsd energies, cm^{-1}		Calcd energies, cm^{-1} ^{a}	Assignment
$E \parallel c$	$E \perp c$		
6 810	6 850		
7 690	7 690	7 250	$^5E(D)$
12 500	12 151	11 995	$^3T_1(H)^a$
15 380	15 385		
		16 801	$^3T_2(H)$
17 990	18 018		
18 700			
19 194			
19 342	19 342		
19 570	19 569		
19 760		19 755	$^3T_1(P)$
	20 202		
20 408	20 421	20 280	$^3T_1(H)^b$
20 534	20 534		
20 661	20 665		
21 186	21 186		
21 277	21 277		
21 505		21 530	$^3T_2(F)$
22 727	22 480	22 410	$^3E(H)$
23 256	23 256		
23 390	23 364		
	23 419		
23 460	23 458		
23 580	23 568		
23 644	23 663		
23 714			
24 155	24 155		
24 390	24 390		
25 400	25 400		
		26 331	$^3T_2(G)$
	27 500	27 116	$^3A_2(F)$
		27 399	$^3T_1(F)$
	28 600	28 048	$^3E(G)$
	30 520	30 550	$^3A_1(G)$

[a] $Dq = 725\ cm^{-1}$; $B = 900\ cm^{-1}$; $C = 3800\ cm^{-1}$.

cillator strength of this absorption in the materials studied is given in Table IV. Also presented in Table IV are the measured oscillator strengths of the $^5T \rightarrow {}^3\Gamma$ manifolds described in the remainder of this section.

The second major region of absorption lies between ~10000 and 13000 cm⁻¹. It contains a broad, weak manifold in both polarizations. The oscillator strength of the $E \perp c$ component is about twice that of the $E \parallel c$ component in all of the spectra.

The third region extends from ~13000 to 17000 cm⁻¹. It contains a broad, asymmetric, fairly intense manifold. The oscillator strength of the $E \parallel c$ absorption is approximately twice that of the $E \perp c$ absorption. In $CsFeCl_3$ this manifold resolves at 4.2 K into a low-energy shoulder and three peaks on the band top. The spacing between the three peaks is ~240 cm⁻¹. These may be components of a vibrational progression corresponding to the 245-cm⁻¹, E_{1u}, infrared-active mode reported for $CsFeCl_3$.[29] This is the only progression observed in any of the $AFeX_3$ spectra.

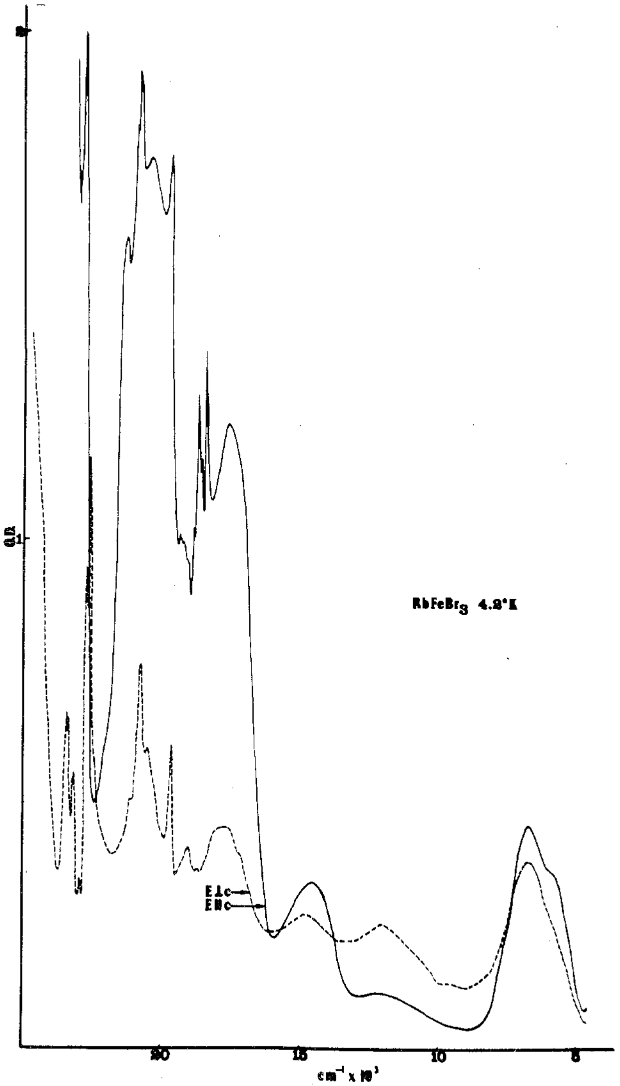

Figure 1. Polarized, single-crystal absorption spectrum of $RbFeBr_3$ at 4.2 K (optical density in arbitrary units).

The higher energy regions of these spectra are well resolved only at 4.2 K. At room temperature the region above 17000

Table IV. $AFeX_3$ Oscillator Strengths ($f \times 10^5$) at 4.2 K

Assigned components	Manifold center, cm^{-1}		$CsFeBr_3$	$RbFeBr_3$	$CsFeCl_3$	$RbFeCl_3$	$CsMg_{0.88}Fe_{0.12}Cl_3$
$^5E(D)$	~7 000	$E \parallel c$	3.64	1.78	4.06	4.62	3.97
		$E \perp c$	1.82	1.27	2.12	2.62	2.15
$^3T_1(H)^a$	~12 300	$E \parallel c$	0.18	0.12	0.06	0.15	0.16
		$E \perp c$	0.32	0.37	0.22	0.36	0.15
$^3T_2(H)$ $^3T_2(F)$ $^3E(H)$	~15 000	$E \parallel c$	0.42	0.60	0.66	1.23	0.35
		$E \perp c$	0.19	0.17	0.17	0.43	0.22
$^3T_1(P)$ $^3T_1(H)^b$ $^3T_2(F)$ $^3E(H)$	~20 000	$E \parallel c^a$	~9.5	~11	~6	~8.5	~2.5
		$E \perp c^a$	~1	~2	~0.5	~0.5	~1
	~23 000	$E \parallel c$			0.65		0.19
$^3\Gamma(G)$		$E \perp c$	0.49	0.89	0.17	0.15	0.11
$^3T_2(G)$	~24 000	$E \parallel c$					
		$E \perp c$	0.27	0.26	0.08	0.16	

[a] Overlap with adjacent d–d bands and the charge-transfer absorption negates the significant-figure accuracy of these measurements; however, relative values and magnitudes are significant.

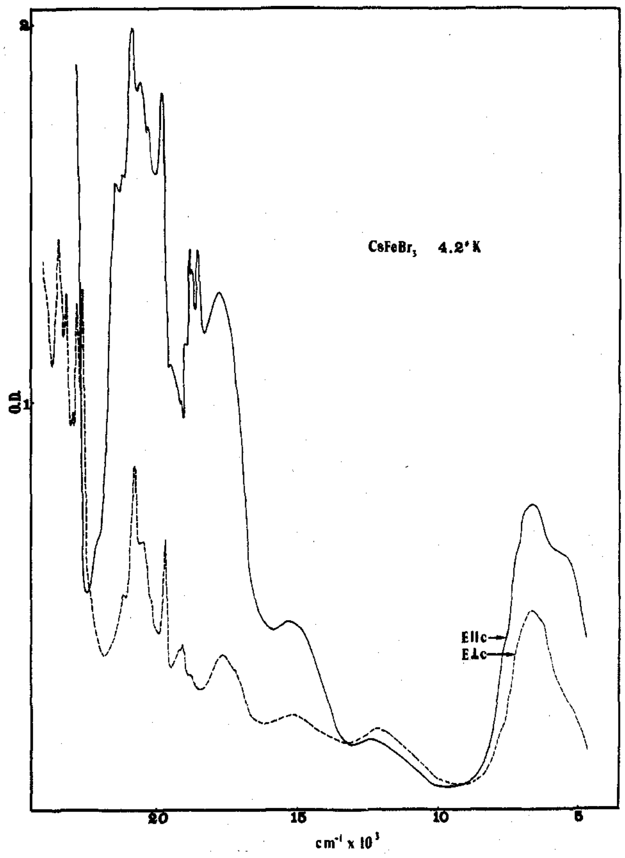

Figure 2. Polarized, single-crystal absorption spectrum of $CsFeBr_3$ at 4.2 K (optical density in arbitrary units).

cm^{-1} appears as a broad shoulder on the charge-transfer band. Partial resolution of some components in this region begins at 150 K. The fourth region lies between ~17000 and 22500 cm^{-1}. It contains a series of four intense, strongly overlapped bands in the pure systems and four much less intense absorptions in the dilute samples. In all cases in the pure systems the $E \parallel c$ absorptions are some 10–20 times more intense than the $E \perp c$ counterparts. The $E \parallel c$ bands are ~5 times more intense in the dilute samples.

The fifth region extends from ~22500 cm^{-1} to the charge-transfer absorption edge. The $E \perp c$ spectra contain two absorption manifolds in this region. The first manifold near 23000 cm^{-1} is resolved at 4.2 K into three sharp components in $CsFeCl_3$ and $RbFeCl_3$, two sharp components in $RbFeBr_3$ and $CsFeBr_3$, four sharp, weak components in $CsMg_{0.88}Fe_{0.12}Cl_3$, and a single, extremely weak absorption in $CsMg_{0.95}Fe_{0.05}Cl_3$. In all but the 5% sample these are the sharpest absorptions in the spectra. The manifold increases in oscillator strength by ~50% as the temperature is lowered from 150 to 4.2 K in all spectra but that of the 5% sample. The majority of the increase occurs below 20 K. This absorption is fully resolved in the $E \parallel c$ orientation only in $CsFeCl_3$, $RbFeBr_3$, and the dilute compounds. The second band in this region is observed near 24000 cm^{-1} in the $E \perp c$ spectra. It appears as a rather weak absorption with a low-energy shoulder in $CsFeCl_3$ and $RbFeCl_3$, as two sharp peaks in $CsFeBr_3$ and $RbFeBr_3$, and as two very weak peaks in the 12% sample and is not resolved in the 5% sample. The intensity of this absorption shows a slight increase as the temperature is lowered from 77 to 4.2 K. The $E \parallel c$ component of this band is observed only in $CsFeCl_3$ and the 12% sample. Overlap with the charge-transfer edge obscures this band in the other $E \parallel c$ spectra.

In the spectra of the pure compounds the charge-transfer absorption edge begins to dominate the spectrum at ~24000 cm^{-1} with $E \parallel c$ and at ~25000 cm^{-1} with $E \perp c$. In the dilute samples the $E \parallel c$ charge-transfer edge is observed at ~25000 cm^{-1}. In the $E \perp c$ orientation the charge transfer in the dilute systems is less intense and much broader than the previous cases. In this orientation two additional absorptions are found near 25750 and 29500 cm^{-1}.

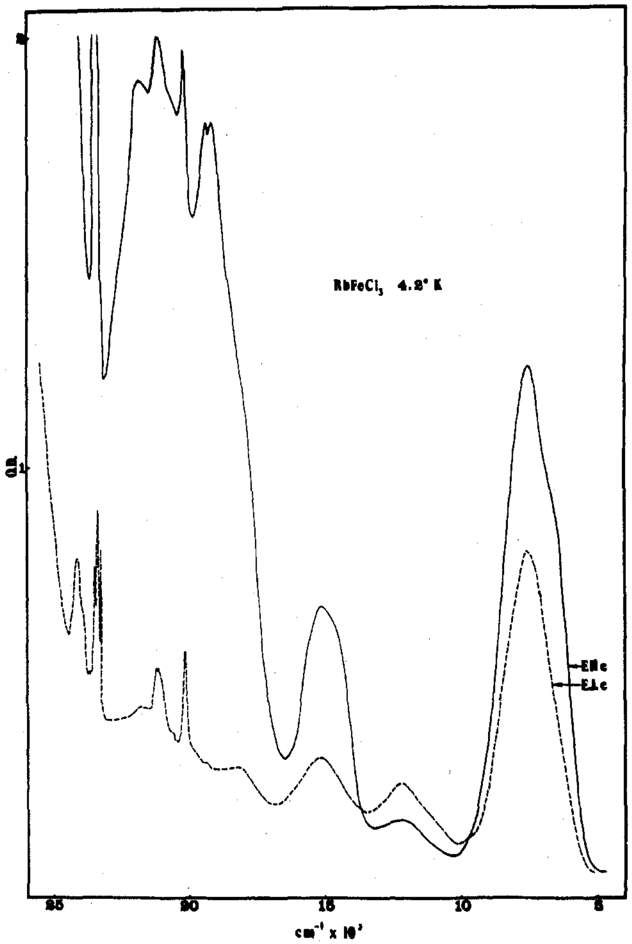

Figure 3. Polarized, single-crystal absorption spectrum of $RbFeCl_3$ at 4.2 K (optical density in arbitrary units).

The oscillator strengths of the absorptions between 10000 and 22500 cm^{-1} in the pure samples appear to increase by ~10% as the temperature is lowered from 150 to 77 K and then to decrease by the same amount as the temperature is further lowered to 4.2 K. These measurements were complicated by overlap between adjacent bands and overlap with the charge-transfer absorption. The estimations involved negate the absolute readings but the trend in oscillator strength as temperature is lowered is valid.

The absorptions above 10000 cm^{-1} are dependent on concentration. The spectrum of the dilute sample containing 12% iron(II) contains all of the absorptions present in the spectra of the pure systems. In the case of the 5% sample the limits of our apparatus allowed spectral measurement of a 5 mm thick crystal which was insufficient to resolve all absorptions.

Finally, the axial spectrum of all compounds was measured and found to be identical with the $E \perp c$ measurements.

Assignment of the Spectra

The major absorption regions of the $AFeX_3$ spectra can be accounted for by considering the $^5T_2(D) \rightarrow {}^5E(D)$ transition and the numerous triplet, ligand field states of the d^6 electronic configuration. The measured spectra were assigned by comparison with energies obtained from the computer diagonalization of the weak-field, octahedral, d^6 matrices given

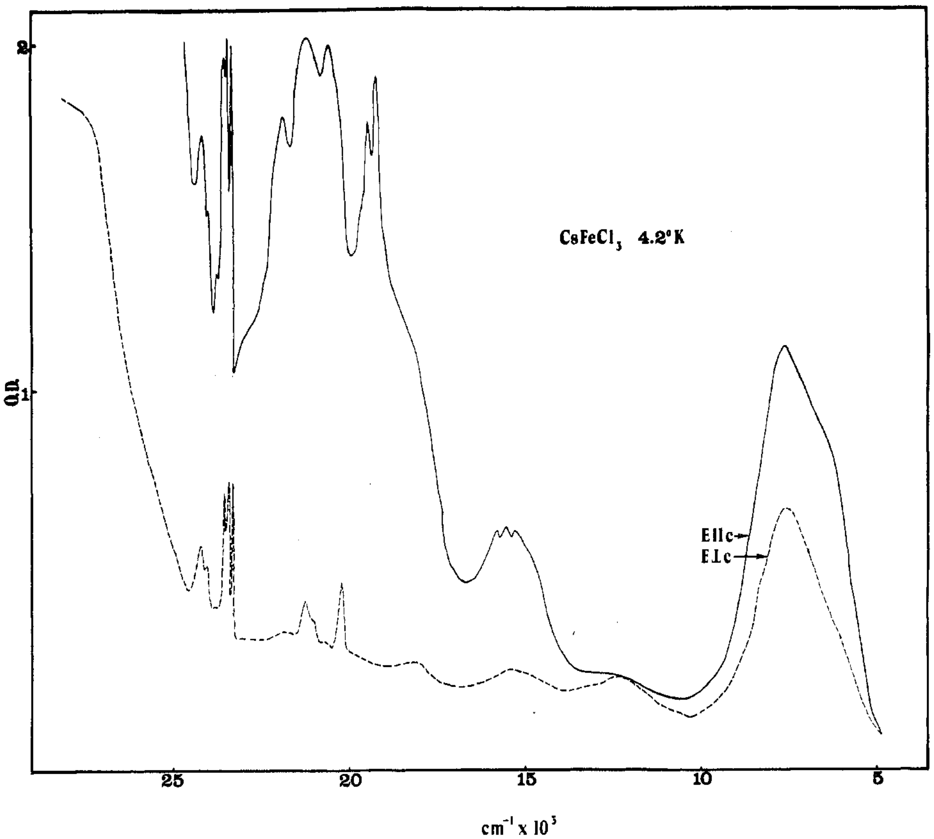

Figure 4. Polarized, single-crystal absorption spectrum of CsFeCl$_3$ at 4.2 K (optical density in arbitrary units).

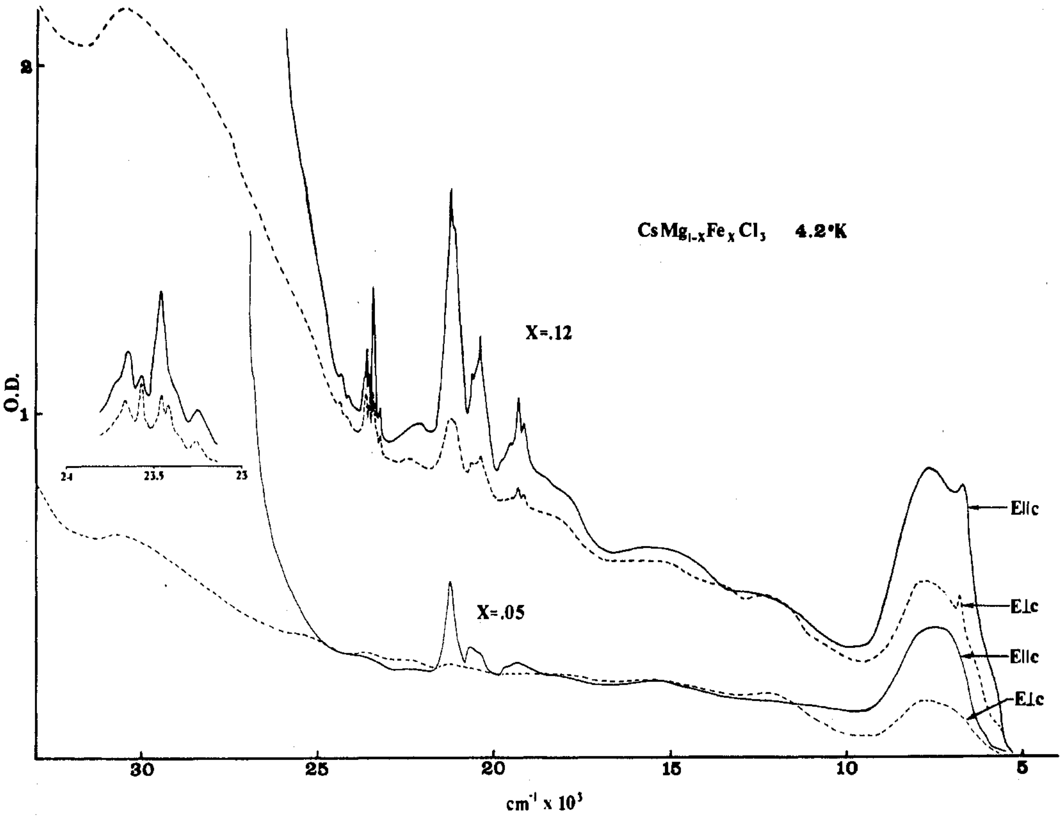

Figure 5. Polarized, single-crystal absorption spectra of CsMg$_{0.88}$Fe$_{0.12}$Cl$_3$ and CsMg$_{0.95}$Fe$_{0.05}$Cl$_3$ at 4.2 K (optical density in arbitrary units).

by Ferguson et al.[22] together with weak-field term energies given by Slater.[30] These matrices include only the triplet states and do not include spin–orbit coupling. The crystal field strength, *Dq*, and Racah interelectron repulsion parameters, *B* and *C*, were estimated from experimental results and input as variables. The calculated energies were then compared with observed energies until a best fit was obtained. The results are listed in Tables I–III.

While this method proved useful in assigning some transitions, it clearly does not accurately account for all manifolds nor does it account for splittings and structure observed in the regions above ~17000 cm^{-1}. Konig and Kremer[31] have published the results of the complete ligand field, Coulomb-repulsion, spin–orbit interaction calculation of the energy levels for the d^6 electronic configuration in an octahedral field. This work indicates that the calculated state labeled $^3T_2(H)$ in our tables is ~1000 cm^{-1} too high and that the state labeled $^3T_2(G)$ has components some 2000 cm^{-1} lower in the complete calculation. These differences account for two major discrepancies between our calculation and measured spectra. The complete calculation also indicates that there is considerable splitting and state mixing in the region between ~17500 and ~21500 cm^{-1} which likely accounts for the additional peaks we have observed in this region.

As Konig and Kremer did not publish the matrix elements with their diagram, no comparative calculation was made using the matrices which include spin–orbit coupling. We should also point out that the diagram furnished by Ferguson et al.[22] with their matrices appears to be incorrect. Because of the manner of computation in that work, it was unclear from where the discrepancy arose. We have recalculated the matrices they presented and found them to be correct. Therefore, it appears that the three low-lying triplet states are incorrectly drawn in their diagram. The present labeling of $^3T_1(P)$, $^3T_2(H)$, $^3T_1(H)$ lowest to highest for the three low triplets should be revised to $^3T_1(H)$, $^3T_2(H)$, $^3T_1(P)$ to make the diagram useful.

In addition to spin–orbit coupling, it is possible that some of the observed splitting may be due to the actual D_{3d} site symmetry of the metal ion. In D_{3d} the octahedral T_1 state is split into A_2 and E components while the T_2 is split into an A_1 and E. Likewise in the D_3 double group the octahedral Γ_4 is split into Γ_2 and Γ_3, and Γ_5 is split into Γ_1 and Γ_3. While this effect most likely makes some contribution to the observed splitting, the absence of clear-cut polarization behavior in the measured spectra makes unambiguous analysis on this basis impossible.

A final consideration concerns the structured absorption manifold observed near 23000 cm^{-1} in all of the spectra and arises from transitions to spin–orbit components of ^3G. This absorption manifold shows a large increase in oscillator strength as the temperature is lowered with the major portion of increase occurring between 20 and 4.2 K. The lack of total resolution above 20 K makes it impossible to follow individual components as temperature is varied. The behavior at least suggests the presence of magnon cold-band character in this absorption.

Discussion

The most notable features of the spectra of the linear-chain $AFeX_3$ compounds are the intensity of the formally spin-forbidden transitions and the overall similarity of the spectra. The enhanced intensity makes available for study a large number of transitions which are not normally observed, while the similarities of the spectra aid in the spectral assignments and lend generality to the conclusions.

The oscillator strength of the spin-allowed $^5T_2(D) \rightarrow {}^5E(D)$ transition is on the order of 10^{-5} in all compounds, as expected. The spin-forbidden transitions in the pure compounds possess oscillator strengths ranging from 10^{-6}, for some transitions, to 10^{-5} for the transitions between ~17000 and 22500 cm^{-1}. For comparison, the oscillator strength of a spin-forbidden transition occurring in a metal ion in solution is on the order of 10^{-9}. Therefore, the spin-forbidden transitions in the linear-chain $AFeX_3$ compounds are enhanced by three to four orders of magnitude relative to those of isolated complexes and in some cases reach the intensity of spin-allowed transitions. In the dilute system the spin-forbidden transitions are also enhanced but by one to three orders of magnitude less than the pure systems. The spin-forbidden transitions in the 12% sample are less intense by one order of magnitude and those in the 5% sample less by two to three orders of magnitude.

Enhancement of this magnitude cannot be accounted for by single-complex, spin–orbit coupling and the temperature dependence of the oscillator strengths is not indicative of a vibronic interaction. It appears that a cooperative mechanism involving adjacent transition metal ions is dominant in these systems. Such a mechanism would account for the concentration dependence of the enhancement in that the dilute samples would contain fewer adjacent metal ions. Similar enhancement has been observed in certain lattices with three-dimensional coupling[32] and a mechanism based on exchange-coupled pairs of metal ions has been postulated in explanation. The specifics of this mechanism have been discussed by several authors.[19,32-43] The result of this mechanism, simply stated, is an exchange-coupled pair state from which magnon–exciton and double-exciton pair transitions can occur. Further, this mechanism results in a single-ion, exchange-induced, electric dipole absorption process which is spin independent.[35,38]

While the relaxation of the spin selection rule by such a process is useful in qualitatively accounting for certain anomalies, it is not a complete explanation. An obvious point in fact is that transitions to states of the same symmetry and spin multiplicity differ in enhancement by as much as an order of magnitude. Indeed, as we discussed in a previous work,[44] it is possible and at times necessary to involve two accepted mechanisms simultaneously to account for observed anomalous behavior. In order to elucidate the correct selection rules and more accurately to understand the interactions in pure salts which lead to such rules and enhancement, it would seem that a broader experimental characterization would be useful.

Lohr and McClure[34] initiated such a characterization based upon their study of a series of three-dimensionally coupled Mn(II) salts. Many of their findings apply in general to the spectra of pure, magnetic salts. The results of this work allow us to expand on their characteristics and add several more. We shall restate the original characterization in general, rather than limit it to the manganese(II) ion from which it derived, and add supportive or opposing evidence from our study. We will then include new characteristics derived from our work. The resulting empirical characterization of a cooperative interaction which is responsible for anomalous optical properties displayed by transition metal containing magnetic salts in the solid state can be summarized as follows.

(1) *Absorption intensity is relatively great whenever the metal ions are separated by a single ligand atom. When more than one ligand atom separates the metal ions, the observed intensity is closer to that of an isolated, single complex as would be the case for a polyatomic ligand like* SO_4^{2-}. In the linear-chain systems where three monoatomic ligand bridges are present the pathway seems even more favorable as evidenced by the strong enhancement dominant along the chain axis. This is further supported by the decreased intensity observed in the dilute sample in which metal ion–metal ion interactions are significantly reduced.

(2) *The cooperative interaction mechanism breaks down spin-forbiddenness more effectively than single-complex spin–orbit coupling.* The spin–orbit induced transition moment necessary to account for oscillator strengths of the order of 10^{-5} for spin-forbidden transitions would be absurdly large for d–d transitions in a centrosymmetric complex.

(3) *The intensity mechanism may destroy parity forbiddenness giving rise to sharp origin bands.* This conclusion was based on a study of Mn(II) spectra in which all transitions

are spin and parity forbidden.[34] In our work, however, direct comparison of spin-allowed and spin-forbidden transitions is possible and the spin-allowed intensity is not observably enhanced. If the parity selection rule were relaxed, enhancement of all d–d adsorptions to a level near that observed in tetrahedral complexes would be expected and this is not the case.

(4) *The cooperative mechanism does not give rise to temperature dependence of the type expected for vibronically assisted transitions described by* $f(T\ K) = f(0\ K) \coth (h\nu/2kT)$ *where* ν *is the frequency of an odd-parity vibration.* In the spectra reported here only the spin-allowed transition displays vibronically assisted temperature dependence.

(5) *The intensity enhancement is not related to the three-dimensional ordering temperature.* The intensities of the pure $AFeX_3$ crystals are anomalously large throughout the measured temperature range indicating that the principal cause of the enhancement is not related to long-range spin correlation. The lowest temperature at which our measurements were taken is 4.2 K and this is below the reported ordering temperature of only one of the studied compounds, $RbFeBr_3$. There is no evidence of any spectral change in the 4.2 K spectrum of $RbFeBr_3$, making it different from the other spectra.

(6) *The cooperative mechanism does not require translationally inequivalent metal ions.* The large enhancements of the translationally equivalent iron complexes observed here certainly support this conclusion but no additional information on this point has been obtained.

(7) *The mechanism may intensify some crystal field bands more than others.* The triplet absorptions between 17000 and 22500 cm^{-1} in $AFeX_3$ spectra are enhanced an order of magnitude more than other triplet absorptions of the same state symmetry.

To this initial characterization we can add the following points.

(8) *The cooperative mechanism does not appreciably alter the crystal field energy levels of the metal ion.* The observed spectra, in terms of band positions, can be assigned according to rules derived for isolated, near-octahedral metal ion complexes. The absorption bands are intensified but not significantly shifted.

(9) *The cooperative mechanism is not dependent on the type of magnetic exchange dominant in the system.* The spectra of intrachain ferromagnetic $RbFeCl_3$ and $CsFeCl_3$ and intrachain antiferromagnetic $RbFeBr_3$ and $CsFeBr_3$ are different in no manner relatable to exchange. The observed differences resulted from the intrinsic difference in crystal field strength of chloride and bromide ligands.

(10) *The cooperative mechanism is dependent to some extent on the bonding pathway.* The spin-forbidden transitions are enhanced more in the $AFeBr_3$ compounds than in the $AFeCl_3$ compounds. This may result from increased orbital availability, increased spin–orbit coupling, or increased polarizability in the bromides.

(11) *The cooperative mechanism is not exclusively the property of pure compounds but is present when aggregates, possibly as small as a pair, exist.* Enhancement is observed in the very dilute compound even though the number of linked ions is statistically small and is seen to increase as the metal ion concentration increases. This corresponds directly to an increasing number of linked metal ions as concentration is increased. Finally, the ease of observation of the enhanced triplet levels over a wide, spectral range makes these measurements the best empirical characterization of the electronic structure of near-octahedral iron(II) thus far obtained. This also suggests that improved characterization of spin-forbidden transitions in other metal ions may be obtained in systems where a cooperative enhancement mechanism is dominant.

Acknowledgment. This work was supported in part by the National Science Foundation (Grant GP-47506) and the Office of Naval Research.

Registry No. $CsFeCl_3$, 15611-69-5; $RbFeCl_3$, 15611-73-1; $CsFeBr_3$, 53899-57-3; $RbFeBr_3$, 37473-39-5; $CsMgCl_3$, 12371-11-8.

References and Notes

(1) On leave from the Department of Chemistry, Florida State University, Tallahassee, Fla. 32306.

(2) For a review of experimental work on these systems see J. F. Ackerman, G. M. Cole, and S. L. Holt, *Inorg. Chim. Acta*, **8**, 323 (1974), and references therein.

(3) R. Dingle, M. E. Lines, and S. L. Holt, *Phys. Rev.*, **187**, 643 (1969).

(4) (a) M. T. Hutchings, G. Shirane, R. J. Birgeneau, and S. L. Holt, *Phys. Rev. B*, **5**, 1999 (1972); (b) R. J. Birgeneau, R. Dingle, M. T. Hutchings, G. Shirane, and S. L. Holt, *Phys. Rev. Lett.*, **26**, 718 (1971).

(5) J. F. Ackerman, E. M. Holt, and S. L. Holt, *J. Solid State Chem.*, **9**, 279 (1974).

(6) G. L. McPherson, T. J. Kistenmacher, J. B. Folkers, and G. D. Stucky, *J. Chem. Phys.*, **57**, 3771 (1972).

(7) T. Li and G. D. Stucky, *Acta Crystallogr., Sect. B*, **29**, 1529 (1973).

(8) P. A. Montano, H. Schechter, E. Cohen, and J. Makovsky, *Phys. Rev. B*, **9**, 1066 (1974).

(9) P. A. Montano, E. Cohen, H. Shechter, and J. Makovsky, *Phys. Rev. B*, **7**, 1180 (1973).

(10) M. Eibschütz, M. E. Lines, and R. C. Sherwood, *Phys. Rev. B*, **11**, 4595 (1975).

(11) M. E. Lines and M. Eibschütz, *Phys. Rev. B*, **11**, 4583 (1975).

(12) S. L. Holt, to be submitted for publication.

(13) O. G. Holmes and D. S. McClure, *J. Chem. Phys.*, **26**, 1686 (1957).

(14) F. A. Cotton and M. D. Meyers, *J. Am. Chem. Soc.*, **82**, 5023 (1960).

(15) W. E. Hatfield and T. S. Piper, *Inorg. Chem.*, **3**, 1295 (1964).

(16) G. D. Jones, *Phys. Rev.*, **155**, 259 (1967).

(17) G. Winter, *Aust. J. Chem.*, **21**, 2859 (1968).

(18) T. E. Freeman and G. D. Jones, *Phys. Rev.*, **182**, 411 (1969).

(19) Y. Tanabe and K.-I., Gondaira, *J. Phys. Soc. Jpn.*, **22**, 573 (1967).

(20) P. G. Russell, D. S. McClure, and J. W. Stout, *Phys. Rev. Lett.*, **16**, 176 (1966).

(21) T. Kambara, *J. Phys. Soc. Jpn.*, **24**, 1242 (1968).

(22) J. Ferguson, H. J. Guggenheim, and E. R. Krausz, *Aust. J. Chem.*, **22**, 1809 (1969).

(23) H.-J. Seifert and K. Klatyk, *Z. Anorg. Allg. Chem.*, **324**, 1 (1966).

(24) G. R. Davidson, M. Eibschutz, D. E. Cox, and V. J. Minkiewitz, *AIP Conf. Proc.*, **No. 5**, 436 (1971).

(25) M. Eibschütz, G. R. Davidson, and D. E. Cox, *AIP Conf. Proc.*, **No. 18**, 386 (1973).

(26) G. L. McPherson, T. J. Kistenmacher, and G. D. Stucky, *J. Chem. Phys.*, **52**, 815 (1970).

(27) E. M. Holt, unpublished results.

(28) C. Simo and S. L. Holt, *J. Solid State Chem.*, **4**, 76 (1972).

(29) G. L. McPherson and J. R. Chang, *Inorg. Chem.*, **12**, 1196 (1973).

(30) J. C. Slater, *Quantum Theory At. Mol., Solid State*, **2**, Appendix 24 (1966).

(31) E. Konig and S. Kremer, *J. Phys. Chem.*, **78**, 56 (1974).

(32) D. D. Sell, R. L. Green, and R. M. White, *Phys. Rev.*, **158**, 489 (1967).

(33) J. Ferguson, H. J. Guggenheim, and Y. Tanabe, *Phys. Rev.*, **161**, 207 (1967).

(34) L. L. Lohr and D. S. McClure, *J. Chem. Phys.*, **49**, 3516 (1968).

(35) J. Ferguson, H. J. Guggenheim, and Y. Tanabe, *J. Appl. Phys.*, **36**, 1046 (1965).

(36) J. Ferguson, H. J. Guggenheim, and Y. Tanabe, *Phys. Rev. Lett.*, **14**, 737 (1965).

(37) Y. Tanabe, T. Moriya, and S. Sugano, *Phys. Rev. Lett.*, **15**, 1023 (1965).

(38) J. Ferguson, H. J. Guggenheim, and Y. Tanabe, *J. Phys. Soc. Jpn.*, **21**, 692 (1966).

(39) J. Ferguson, H. J. Guggenheim, and Y. Tanabe, *J. Chem. Phys.*, **45**, 1134 (1966).

(40) K. Shinagawa and Y. Tanabe, *J. Phys. Soc. Jpn.*, **30**, 1280 (1971).

(41) T. Fujiwara and Y. Tanabe, *J. Phys. Soc. Jpn.*, **32**, 912 (1972).

(42) T. Fujiwara, W. Gebhardt, K. Pentanides, and Y. Tanabe, *J. Phys. Soc. Jpn.*, **33**, 39 (1972).

(43) K. Ebara and Y. Tanabe, *J. Phys. Soc. Jpn.*, **36**, 93 (1974).

(44) G. M. Cole, Jr., C. F. Putnik, and S. L. Holt, *Inorg. Chem.*, **14**, 2219 (1975).